

Adsorption Equilibria of Ammonia Gas on Inorganic and Organic Sorbents at 298.15 K

Jarkko Helminen,* Joni Helenius, and Erkki Paatero

Laboratory of Industrial Chemistry, Lappeenranta University of Technology, P.O. Box 20, FIN-53851 Lappeenranta, Finland

Ilkka Turunen

Laboratory of Process Systems Engineering, Lappeenranta University of Technology, P.O. Box 20, FIN-53851 Lappeenranta, Finland

The adsorption equilibria of ammonia gas on various inorganic and organic sorbents were determined at 298.15 K in a pressure range of 0–101 kPa using a static volumetric apparatus. The zeolite sorbents were 4A, 5A, 13X, dealuminated faujasite, dealuminated pentasil, and clinoptilolite. To illustrate the differences between commercial grades, the 5A and 13X zeolites were obtained from three suppliers. Other inorganic sorbents were three aluminas and three silica gels. Organic sorbents were two activated carbons, charcoal, and two polymeric sorbents (sulfonated and nonsulfonated). The nonlinear experimental equilibrium data were fitted to the Langmuir, Freundlich, Langmuir–Freundlich, and Toth isotherm models. The Henry model was used for the linear equilibrium data. The equilibria of all of the sorbents, with the exception of sulfonated polymeric and dealuminated pentasil zeolite sorbents, provide an accurate correlation with the isotherm models over the entire pressure range.

Introduction

The design of gas adsorption processes is mainly based on the equilibrium of gas compounds on the surface of a sorbent. At present, adsorption equilibria cannot be predicted, e.g., by a molecular simulation, and they have to be measured experimentally for each sorbent. Consequently, the need for extensive experimental work has been an obstacle for the utilization of adsorption technology in industrial separations.^{1–8}

Ammonia gas is one of the most widely used chemicals. Generally, it has to be removed <1 ppm, e.g., from the gaseous effluents of ammonia, fertilizer, and urea plants. Traditionally, ammonia gas effluents have been separated by gas absorbers, which produce a lot of waste solutions and do not allow an effective ammonia recovery.^{9–11} There are also process gas streams where ammonia separation by adsorption and its recovery would be a tempting possibility.¹² However, there is not enough information available for the selection of the most beneficial sorbent for the ammonia separation. Only four references are given for ammonia gas adsorption in Valenzuela and Myers' data handbook¹³ in which the experimental pressure and temperature come up to the levels of industrial ammonia gas streams.^{14–17} These sources include the ammonia equilibria on activated carbon,¹⁴ silica gel,¹⁵ La mordenite, Ru mordenite,¹⁶ and Y zeolite in Na, La, LaH, LaCa, H, and Ca forms.¹⁷ In addition to the above-mentioned data handbook, ammonia equilibria have been determined for the following sorbents: natural zeolites¹⁸ (such as mordenite, erionite, clinoptilolite, phillipsite, and chabazite); NaZSM5 zeolite;¹⁹ 5A zeolite;^{20,21} zeolite A in Li⁺, Na⁺, Ag⁺, Ca²⁺, Sr²⁺, Co²⁺, Ni²⁺, Zn²⁺, and Cd²⁺ forms;²² zeolite Y in Li⁺, Na⁺, K⁺, Ag⁺,

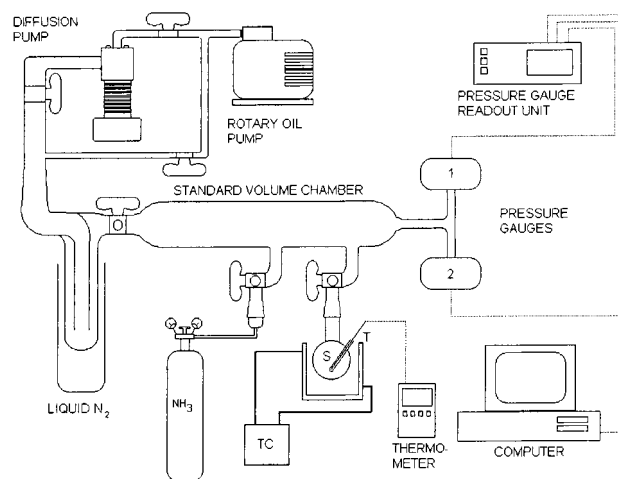


Figure 1. Volumetric adsorption equilibrium apparatus. Diffusion pump (LEYBODIFF 40); rotary oil pump (EDWARDS SPEEDVAC 2); pressure gauge readout unit (LEYBOLD-HERAEUS INFICON CM3); (1) capacitance manometer gauge for 0–1.3332 kPa pressure range (LH INFICON CM100-G10A); (2) capacitance manometer gauge for 0–133.2 kPa pressure range (LH INFICON CM100-G1000A); (T) thermocouple (NiCr–Ni); (TC) temperature-controlled water bath (LAUDA B); (S) glass sample flask; liquid N₂ trap.

Ca²⁺, Sr²⁺, Ba²⁺, Mn²⁺, Co²⁺, and HNa forms;²³ CrL, FeL, CoL, YL, CoX, MnX, CoY, and MnY zeolites;²⁴ activated carbons;²⁵ and polymer fibers in Ni and Cu forms.²⁶ Unfortunately, only a few of the above sources^{15,17,18,24,25} are relevant for design purposes because most of them do not give pure equilibrium data and/or accurate correlations.

Our work for the determination and modeling of ammonia adsorption equilibria has been divided into two parts. The present study reports ammonia adsorption

* Corresponding author. E-mail: Jarkko.Helminen@lut.fi. Fax: +358 5 6212199.

Table 1. Physical Properties of the Sorbents

sorbent	manufacturer/supplier	D^a (mm)	form	$d^{a,b}$ (Å)	BET ^c (m ² g ⁻¹)	ρ_{bulk} (kg m ⁻³)
activated carbon (Aldrich Darco 24,226-8)	Sigma-Aldrich Co.	0.4–0.84	granule		430	359
activated carbon (Merck 1.09624)	Merck KGaA	0.5–1.0	granule		450	436
charcoal (Sigma C 3014)	Sigma Chemical Co.	0.25–0.84	granule		210	239
alumina (Compalox VPO2)	Martinswerk GmbH	1–3	granule	50	264	930
alumina (LaRoche 1593)	LaRoche Industries Inc.	2–3	bead		226	779
alumina (LaRoche 1597)	LaRoche Industries Inc.	2–3	bead		297	735
polymer resin [Macronet (MN) 200]	Purolite International Ltd.	0.3–1	bead	19–950	700	285
polymer resin (Amberlyst 15)	Rohm & Haas Co.	0.3–0.84	bead		225	519
silica gel 40 (Fluka 60736)	Fluka Chemie AG	0.2–0.5	granule	40	469	524
silica gel 60 (Fluka 60742)	Fluka Chemie AG	0.2–0.5	granule	60	450	445
silica gel 100 (Fluka 60746)	Fluka Chemie AG	0.2–0.5	granule	100	238	394
5A zeolite (Baylith KE154)	Bayer AG	1.5–3	bead	5	301	713
4A zeolite (Baylith TG242)	Bayer AG	1–1.6	bead	4		778
13X zeolite (Baylith WE894)	Bayer AG	2–3.5	bead	9	365	647
clinoptilolite [Mud Hills (CA), USA]		0.5–1	granule	3.6		790
5A zeolite (Lancaster 5830)	Lancaster Synthesis	0.4–0.8	bead	5	382	760
13X zeolite (Lancaster 6149)	Lancaster Synthesis	0.4–0.8	bead	8.5	430	682
5A zeolite (Sigma M-5766)	Sigma Chemical Co.	1.4–2.4	bead	5	368	680
13X zeolite (Sigma M-3385)	Sigma Chemical Co.	1.4–2.4	bead	10	462	645
Faujasite dealuminated (Wessalith DAY F20)	Degussa AG	2	cylinder	8	800 ^a	478
Pentasil dealuminated (Wessalith DAZ F20)	Degussa AG	2	cylinder	6	400 ^a	640

^a Data given by supplier. ^b Mean pore diameter. ^c BET single point.

Table 2. Experimental Equilibrium Data for the Alumina Sorbents at 298.15 K

alumina VPO2		alumina 1593		alumina 1597	
p (kPa)	q^* (mmol g ⁻¹)	p (kPa)	q^* (mmol g ⁻¹)	p (kPa)	q^* (mmol g ⁻¹)
0.0011	0.147	0.0157	0.149	0.0225	0.610
0.1772	0.745	0.36	0.731	3.09	1.466
5.19	1.411	5.86	1.226	15.16	2.006
16.59	1.781	17.31	1.512	27.4	2.271
29.2	1.996	28.4	1.662	47.4	2.549
48.7	2.218	47.8	1.849	72	2.807
72.7	2.418	72.7	2.024	98.3	3.008
99.5	2.606	98	2.159		

Table 3. Experimental Equilibrium Data for the Carbon Sorbents at 298.15 K

activated carbon Darco		activated carbon Merck		charcoal Sigma	
p (kPa)	q^* (mmol g ⁻¹)	p (kPa)	q^* (mmol g ⁻¹)	p (kPa)	q^* (mmol g ⁻¹)
6.53	0.781	0.773	0.080	0.547	0.139
17	1.413	3.91	0.270	3.66	0.417
23.4	1.743	8.64	0.514	8.22	0.771
29.5	2.052	17.27	1.005	16.91	1.378
47.1	2.766	26.8	1.559	27	2.000
71	3.521	44.4	2.508	44.8	2.999
96.3	4.192	67.7	3.756	70.1	4.245
		93	5.084	95	5.275

isotherms at 298.15 K on 21 inorganic and organic sorbents, including two activated carbon, three alumina, one charcoal, two polymeric, three silica gel, and 10 zeolite sorbents for use in the selection of the most beneficial sorbents in further studies. The obtained experimental equilibrium data are fitted to five isotherm models in order to evaluate the accuracy of the correlations for design purposes. On the basis of the present work, five sorbents were chosen to evaluate their applicability, especially, in the ammonia separation from the gas streams of urea and melamine plants. The results of the latter work have already been published.²⁷ The selected sorbents were two zeolites (4A Baylith TG242 and 13X Baylith WE894), activated carbon (Merck), alumina (LaRoche 1597), and silica gel (60 Å, Fluka) for which temperature effects and a more extensive theoretical analysis are presented than in the present work. The temperature dependences of

Table 4. Experimental Equilibrium Data for the Silica Gel Sorbents at 298.15 K

silica gel 40		silica gel 60		silica gel 100	
p (kPa)	q^* (mmol g ⁻¹)	p (kPa)	q^* (mmol g ⁻¹)	p (kPa)	q^* (mmol g ⁻¹)
0.0024	0.137	0.0029	0.226	0.0042	0.178
19.07	4.507	0.0842	1.153	0.0835	0.912
72.6	5.835	2.17	2.616	2.84	1.965
96.3	6.250	15.24	3.422	15.85	2.514
		45.2	4.120	27.9	2.761
		94.3	4.855	47.4	3.043
				72	3.356
				97.9	3.602

Table 5. Experimental Equilibrium Data for the Polymeric Sorbents at 298.15 K

Purolite MN200		Amberlyst 15	
p (kPa)	q^* (mmol g ⁻¹)	p (kPa)	q^* (mmol g ⁻¹)
0.316	0.161	0.0071	0.376
2.94	0.534	0.0113	1.114
7.69	0.930	0.0265	2.327
16.57	1.497	0.0743	4.724
26.7	2.050	5.89	7.625
44.7	2.933	33.4	9.563
69	4.086	64.8	10.665
93	5.203	93.4	11.346

Table 6. Experimental Equilibrium Data for the Dealuminated and Natural Zeolites at 298.15 K

faujasite DAY		pentasil DAZ		clinoptilolite	
p (kPa)	q^* (mmol g ⁻¹)	p (kPa)	q^* (mmol g ⁻¹)	p (kPa)	q^* (mmol g ⁻¹)
0.359	0.258	0.0041	0.150	0.002	0.651
5.22	0.471	1.58	0.572	0.0083	2.034
9.28	0.558	7.31	0.883	1.99	4.362
18.78	0.718	27.3	1.446	22.6	5.224
28.4	0.875	80.7	2.347	46.8	5.537
47.4	1.115			72.4	5.753
71.6	1.431			97.9	5.904
97.4	1.778				

equilibria are required in the design of adsorption processes, but the equilibrium data at one temperature as in the present work are often adequate in the preliminary sorbent selection, because the determination of temperature dependences for a large number of sorbents is not, in practice, economically reasonable.

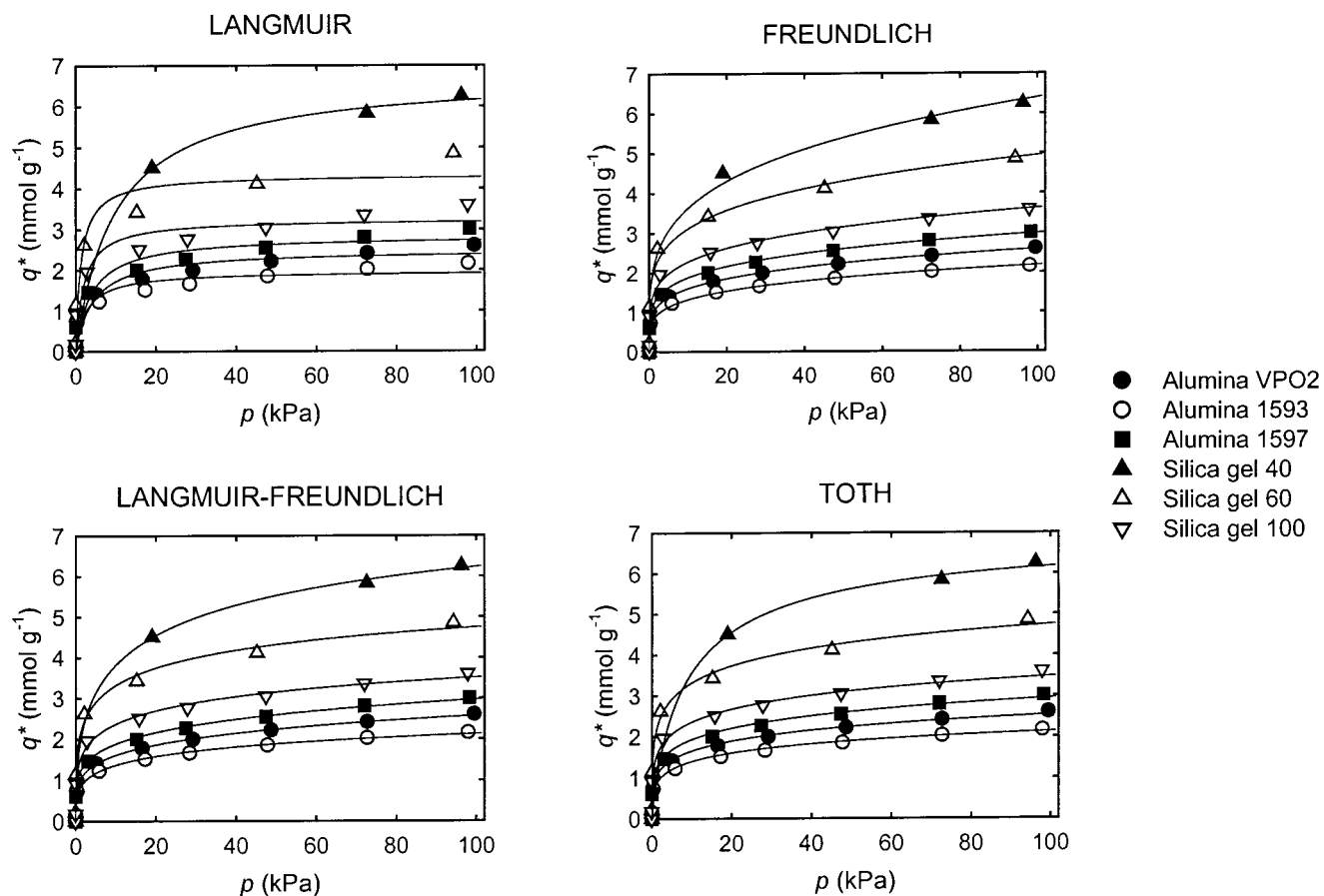


Figure 2. Experimental and predicted ammonia sorbate concentrations at equilibrium on the alumina and silica gel sorbents.

Table 7. Experimental Equilibrium Data for the Synthetic Zeolites (Baylith) at 298.15 K

4A zeolite TG242		5A zeolite KE154		13X zeolite WE894	
p (kPa)	q^* (mmol g ⁻¹)	p (kPa)	q^* (mmol g ⁻¹)	p (kPa)	q^* (mmol g ⁻¹)
0.0009	0.756	0.0008	0.622	0.0011	0.539
0.0171	2.039	0.0058	1.864	0.0041	1.742
0.328	4.564	0.114	4.337	0.1016	4.161
8.53	7.229	11.112	6.662	11.65	7.785
40.6	8.302	45.6	7.289	8.53	7.706
72.6	8.532	72.3	7.503	40.2	8.793
97.8	8.717	97.6	7.674	64	8.939
				93.8	9.326

Experimental Section

Adsorption equilibrium data were measured for the sorbents listed in Table 1 at 298.15 K in a pressure range of 0–101 kPa. Prior to measurement, the sorbent samples were predried overnight at the following temperatures: zeolites and aluminas at 573 K, silica gels at 473 K, polymers at 388 K, and carbons at 473 K. Ultrapure ammonia gas (99.999% by AGA, Sweden) was used without further purification.

Adsorption equilibrium experiments were carried out by a static volumetric method. Figure 1 shows the experimental apparatus made up of glass. The equilibrium isotherm was determined by the following procedure. A sample flask with the precisely weighed sorbent (about 4 g) was connected to the system, and the glass chamber was evacuated to <0.1 Pa. For degasification, the sorbent sample was heated to the same temperature as that in the predrying described above and evacuated for 1 h. The degasified sample was cooled to the measuring temperature at a

Table 8. Experimental Equilibrium Data for the Synthetic Zeolites (Lancaster and Sigma) at 298.15 K

5A zeolite Lancaster		13X zeolite Lancaster	
p (kPa)	q^* (mmol g ⁻¹)	p (kPa)	q^* (mmol g ⁻¹)
0.0008	1.319	0.001	1.264
0.0126	3.206	0.058	3.786
0.83	5.680	2.03	6.694
19.3	6.942	17.8	8.157
45.7	7.362	43.7	8.806
73.7	7.636	72.1	9.115
97.7	7.815	97.4	9.326

5A zeolite Sigma		13X zeolite Sigma	
p (kPa)	q^* (mmol g ⁻¹)	p (kPa)	q^* (mmol g ⁻¹)
0.0085	2.460	0.0018	0.623
0.442	4.868	0.0115	2.489
8.71	6.259	0.302	4.939
25.4	6.750	13.4	6.971
37.8	6.965	32.1	7.881
48.7	7.089	46.3	8.314
72.7	7.276	70.9	8.725
98.7	7.430	96.7	9.030

pressure of <0.1 Pa. Before ammonia was introduced to the system, the standard volume chamber was disconnected from the pumps and the sample flask. Then, ammonia was introduced to the chamber, and the pressure was raised with ammonia to a selected value between 1.2 and 10.0 kPa. At the desired pressure, the valve to the sample flask was opened, after which the pressure decrease was recorded when the equilibrium pressure was achieved. To determine the successive isotherm points, the pressure raising and equilibrating steps were repeated. After the final point near the atmospheric pressure was reached, the

Table 9. Regression Results for the Alumina and Silica Gel Sorbents

sorbent	Langmuir	Freundlich	Langmuir–Freundlich	Toth
alumina VPO2 total SS 7.561	$R^2 = 92.49\%$ RSS = 0.568 SEE = 0.285 $q_s = 2.49 \pm 0.21$ $b = 0.226 \pm 0.116$	$R^2 = 99.84\%$ RSS = 0.012 SEE = 0.042 $K = 0.990 \pm 0.026$ $n = 0.209 \pm 0.007$	$R^2 = 99.85\%$ RSS = 0.011 SEE = 0.043 $q_s = 20.6 \pm 27.0$ $b = 0.0504 \pm 0.0694$ $n = 0.226 \pm 0.026$	$R^2 = 99.77\%$ RSS = 0.017 SEE = 0.054 $q_s = 28.1 \pm 35.8$ $b = 0.299 \pm 0.025$ $n = 0.0786 \pm 0.0342$
alumina 1593 total SS 5.067	$R^2 = 91.85\%$ RSS = 0.413 SEE = 0.243 $q_s = 1.97 \pm 0.15$ $b = 0.381 \pm 0.231$	$R^2 = 99.17\%$ RSS = 0.042 SEE = 0.078 $K = 0.803 \pm 0.045$ $n = 0.217 \pm 0.014$	$R^2 = 99.42\%$ RSS = 0.029 SEE = 0.070 $q_s = 4.89 \pm 2.28$ $b = 0.196 \pm 0.110$ $n = 0.297 \pm 0.056$	$R^2 = 99.52\%$ RSS = 0.024 SEE = 0.063 $q_s = 9.00 \pm 7.71$ $b = 0.342 \pm 0.043$ $n = 0.123 \pm 0.054$
alumina 1597 total SS 8.054	$R^2 = 92.53\%$ RSS = 0.602 SEE = 0.317 $q_s = 2.84 \pm 0.22$ $b = 0.256 \pm 0.123$	$R^2 = 99.90\%$ RSS = 0.008 SEE = 0.036 $K = 1.18 \pm 0.02$ $n = 0.202 \pm 0.005$	$R^2 = 99.86\%$ RSS = 0.011 SEE = 0.048 $q_s = 36.9 \pm 87.8$ $b = 0.0331 \pm 0.0810$ $n = 0.211 \pm 0.028$	$R^2 = 99.51\%$ RSS = 0.040 SEE = 0.089 $q_s = 48.0 \pm 127$ $b = 0.283 \pm 0.038$ $n = 0.0675 \pm 0.0544$
silica gel 40 total SS 37.47	$R^2 = 99.87\%$ RSS = 0.047 SEE = 0.125 $q_s = 6.75 \pm 0.17$ $b = 0.104 \pm 0.014$	$R^2 = 99.50\%$ RSS = 0.186 SEE = 0.249 $K = 2.06 \pm 0.29$ $n = 0.246 \pm 0.033$	$R^2 = 99.98\%$ RSS = 0.009 SEE = 0.068 $q_s = 9.65 \pm 1.18$ $b = 0.234 \pm 0.025$ $n = 0.446 \pm 0.061$	$R^2 = 99.89\%$ RSS = 0.040 SEE = 0.142 $q_s = 7.12 \pm 3.22$ $b = 4.43 \pm 22.10$ $n = 0.786 \pm 1.370$
silica gel 60 total SS 22.09	$R^2 = 93.13\%$ RSS = 1.518 SEE = 0.551 $q_s = 4.33 \pm 0.38$ $b = 0.749 \pm 0.455$	$R^2 = 98.81\%$ RSS = 0.264 SEE = 0.230 $K = 1.96 \pm 0.14$ $n = 0.201 \pm 0.018$	$R^2 = 99.39\%$ RSS = 0.135 SEE = 0.183 $q_s = 7.98 \pm 2.58$ $b = 0.345 \pm 0.162$ $n = 0.314 \pm 0.065$	$R^2 = 99.57\%$ RSS = 0.095 SEE = 0.154 $q_s = 14.2 \pm 9.4$ $b = 0.293 \pm 0.033$ $n = 0.134 \pm 0.056$
silica gel 100 total SS 14.83	$R^2 = 92.76\%$ RSS = 1.073 SEE = 0.392 $q_s = 3.25 \pm 0.23$ $b = 0.502 \pm 0.276$ q_s (mmol g ⁻¹) b (kPa ⁻¹)	$R^2 = 99.07\%$ RSS = 0.137 SEE = 0.140 $K = 1.43 \pm 0.08$ $n = 0.202 \pm 0.015$ K (kPa ⁻¹) n (-)	$R^2 = 99.35\%$ RSS = 0.096 SEE = 0.127 $q_s = 7.52 \pm 3.37$ $b = 0.241 \pm 0.138$ $n = 0.280 \pm 0.055$ q_s (mmol g ⁻¹) b (kPa ⁻¹) n (-)	$R^2 = 99.49\%$ RSS = 0.076 SEE = 0.112 $q_s = 17.6 \pm 18.2$ $b = 0.288 \pm 0.031$ $n = 0.102 \pm 0.056$ q_s (mmol g ⁻¹) b (kPa ⁻¹) n (-)

adsorbed amount of ammonia was calculated based on the measured pressure differences, experimental temperature, and system volumes.

Several experiments for various sorbents were made to obtain the repeatability of isotherm determination. The largest deviation of independently determined equilibria is about 4%, e.g., for the 5A zeolite KE154, but the deviation was usually much lower, e.g., <0.4% for the Lancaster 13X zeolite. Thus, the total error of isotherm determination is slightly smaller compared to the error of $\pm 5\%$ reported previously by Berlier and Frère.²⁸ Individual errors related to the isotherm determinations are those of weight, temperature, and pressure. Sorbent samples were weighed with an accuracy of ± 0.1 mg. The errors of temperature control and indication are ± 0.01 K and 0.5% of range, respectively. The accuracy of the pressure gauges is about 0.5% of the reading.

Results and Discussion

Equilibrium Data. Ammonia adsorption isotherms were obtained for three carbon, three alumina, two polymeric, three silica gel, and 10 zeolite sorbents at 298.15 K covering a pressure range of 0–101 kPa. Tables 2–8 show the experimental equilibrium data. The sulfonated polymeric sorbent Amberlyst 15 has the highest sorbate concentration (about 11.3 mmol g⁻¹) in the vicinity of atmospheric pressure. In contrast, the nonsulfonated polymeric sorbent MN200 has, at the same pressure, a considerably lower sorbate concentration (5.2 mmol g⁻¹). The carbon sorbents, with the exception of the activated carbon

Darco, have approximately the same sorbate concentration as MN200. The sorbate concentrations for carbons compare favorably with the value of 3.5 mmol g⁻¹ at 80 kPa reported by Boki et al.¹⁴ The 4A, 5A, and 13X zeolites give the second highest sorbate concentrations near the upper limit of the pressure range. The 13X zeolites from the three different suppliers provide sorbate concentrations of the same magnitude, namely, 9.0–9.3 mmol g⁻¹. The three different grades of 5A zeolites also adsorb ammonia at 97–98 kPa in almost similar amounts (7.4–7.8 mmol g⁻¹). However, Schirmer et al.²⁰ have obtained higher sorbate concentrations for a binder-free 5A zeolite at 296 K, for example, about 8.7 mmol g⁻¹ at 100 kPa. Hayhurst¹⁸ gives a correlation in order to calculate the sorbate concentrations of three clinoptilolite grades. The correlation predicts sorbate concentrations of 4.3–5.2 mmol g⁻¹, which are lower than the concentration for clinoptilolite (5.9 mmol g⁻¹) in the present work. Among the zeolites, the dealuminated faujasite and pentasil provide the poorest sorbate concentrations, being about 1.8 and 2.3 mmol g⁻¹, respectively. The sorbate concentrations of alumina sorbents are also low (2.2–3.0 mmol g⁻¹). For silica gels, we can observe an increasing sorbate concentration with decreasing pore diameter, and the highest concentration is 6.3 mmol g⁻¹ found for silica gel 40. Kuo et al.¹⁵ have previously measured a higher sorbate concentration, i.e., 6.39 mmol g⁻¹ for the Davison silica gel ($d_{\text{pore}} = 140$ Å, BET 340 m² g⁻¹) at 298 K and 2.7 kPa.

Isotherm Models. Five isotherm models were used to correlate the experimental adsorption equilibrium data. More than one model is required because there is no

Table 10. Regression Results for the Dealuminated, Natural, and Synthetic (Baylith) Zeolites

sorbent	Langmuir	Freundlich	Langmuir–Freundlich	Toth
faujasite DAY total SS 2.567	$R^2 = 93.69\%$ RSS = 0.162 SEE = 0.152 $q_s = 2.31 \pm 0.38$ $b = 0.0251 \pm 0.0095$	$R^2 = 98.26\%$ RSS = 0.045 SEE = 0.080 $K = 0.184 \pm 0.029$ $n = 0.485 \pm 0.039$	$R^2 = 98.19\%$ RSS = 0.046 SEE = 0.088 $q_s = 57.6 \pm 1170.0$ $b = 0.00315 \pm 0.0632$ $n = 0.493 \pm 0.184$	$R^2 = 97.11\%$ RSS = 0.074 SEE = 0.111 $q_s = 24.4 \pm 161.0$ $b = 1.90 \pm 2.82$ $n = 0.206 \pm 0.425$
pentasil DAZ total SS 3.872	$R^2 = 94.70\%$ RSS = 0.205 SEE = 0.226 $q_s = 2.67 \pm 0.41$ $b = 0.0624 \pm 0.0297$	$R^2 = 99.43\%$ RSS = 0.022 SEE = 0.074 $K = 0.424 \pm 0.043$ $n = 0.386 \pm 0.026$	$R^2 = 99.38\%$ RSS = 0.024 SEE = 0.089 $q_s = 57.8 \pm 793.0$ $b = 0.0073 \pm 0.0997$ $n = 0.396 \pm 0.139$	$R^2 = 98.87\%$ RSS = 0.044 SEE = 0.121 $q_s = 62.1 \pm 526.0$ $b = 0.911 \pm 0.778$ $n = 0.127 \pm 0.282$
clinoptilolite total SS 40.97	$R^2 = 96.52\%$ RSS = 1.426 SEE = 0.488 $q_s = 5.37 \pm 0.22$ $b = 71.3 \pm 25.6$	$R^2 = 96.70\%$ RSS = 1.351 SEE = 0.475 $K = 3.37 \pm 0.25$ $n = 0.131 \pm 0.019$	$R^2 = 98.95\%$ RSS = 0.430 SEE = 0.293 $q_s = 6.53 \pm 0.71$ $b = 1.63 \pm 0.73$ $n = 0.336 \pm 0.071$	$R^2 = 99.15\%$ RSS = 0.348 SEE = 0.264 $q_s = 7.01 \pm 1.07$ $b = 0.132 \pm 0.019$ $n = 0.231 \pm 0.069$
4A zeolite TG242 total SS 94.13	$R^2 = 96.02\%$ RSS = 3.747 SEE = 0.790 $q_s = 8.25 \pm 0.41$ $b = 4.46 \pm 1.81$	$R^2 = 97.36\%$ RSS = 2.486 SEE = 0.644 $K = 4.65 \pm 0.34$ $n = 0.149 \pm 0.018$	$R^2 = 99.98\%$ RSS = 0.023 SEE = 0.067 $q_s = 9.82 \pm 0.16$ $b = 1.29 \pm 0.07$ $n = 0.385 \pm 0.012$	$R^2 = 99.97\%$ RSS = 0.027 SEE = 0.073 $q_s = 11.3 \pm 0.4$ $b = 0.184 \pm 0.004$ $n = 0.236 \pm 0.013$
5A zeolite KE154 total SS 73.81	$R^2 = 96.61\%$ RSS = 2.501 SEE = 0.646 $q_s = 7.25 \pm 0.32$ $b = 17.2 \pm 6.8$	$R^2 = 95.90\%$ RSS = 3.025 SEE = 0.710 $K = 4.39 \pm 0.36$ $n = 0.132 \pm 0.020$	$R^2 = 99.66\%$ RSS = 0.254 SEE = 0.226 $q_s = 7.72 \pm 0.23$ $b = 3.27 \pm 0.82$ $n = 0.461 \pm 0.053$	$R^2 = 99.82\%$ RSS = 0.129 SEE = 0.161 $q_s = 8.17 \pm 0.29$ $b = 0.117 \pm 0.008$ $n = 0.319 \pm 0.037$
13X zeolite WE894 total SS 118.1	$R^2 = 96.55\%$ RSS = 4.076 SEE = 0.763 $q_s = 8.55 \pm 0.35$ $b = 10.2 \pm 3.7$ q_s (mmol g ⁻¹) b (kPa ⁻¹)	$R^2 = 96.93\%$ RSS = 3.629 SEE = 0.720 $K = 5.00 \pm 0.36$ $n = 0.150 \pm 0.019$ K (kPa ⁻¹) n (-)	$R^2 = 99.60\%$ RSS = 0.469 SEE = 0.280 $q_s = 10.3 \pm 0.6$ $b = 1.44 \pm 0.35$ $n = 0.376 \pm 0.044$ q_s (mmol g ⁻¹) b (kPa ⁻¹) n (-)	$R^2 = 99.79\%$ RSS = 0.246 SEE = 0.203 $q_s = 11.5 \pm 0.9$ $b = 0.165 \pm 0.010$ $n = 0.239 \pm 0.032$ q_s (mmol g ⁻¹) b (kPa ⁻¹) n (-)

universal equilibrium model which provides an accurate fit for all sorbents. For inorganic and polymeric sorbents, the equilibrium data were fitted to four nonlinear models. The data for the activated carbon Darco and the charcoal Sigma were fitted to nonlinear models as well as to the Henry model because the equilibria are close to linear. The equilibrium of the activated carbon Merck is entirely linear, and only the linear Henry model was used.

For nonlinear equilibrium data, the simplest models are the Langmuir and the Freundlich equations, because they include only two parameters. The thermodynamical basis and use of the Langmuir model for adsorption equilibria is widely accepted.²⁹ The Langmuir model is written as

$$q^* = \frac{q_s b p}{1 + b p} \quad (1)$$

where q^* is the sorbate concentration at equilibrium, q_s is the saturation limit of the sorbate concentration, and b is the adsorption equilibrium constant. At low sorbate concentrations, the Langmuir model follows Henry's law (see eq 5).

Although the Freundlich model can be derived from thermodynamical arguments, it is generally classified to an empirical equation^{2,3}

$$q^* = K p^n \quad (2)$$

where K is the Freundlich constant and n is an empirical exponent.

Two three-parameter nonlinear models were considered in this work. Like the Freundlich model above, the Langmuir–Freundlich model is also an empirical model without a solid thermodynamical base.² However, the Langmuir–Freundlich model, known also as the Sips model, is widely used, because it can model a wide variety of sorption data³⁰

$$q^* = \frac{q_s b p^n}{1 + b p^n} \quad (3)$$

Both the Freundlich and Langmuir–Freundlich models do not follow Henry's law at low concentrations, which is commonly regarded as a condition for thermodynamical consistency.

The Toth model has been considered a pure empirical model³⁰

$$q^* = \frac{q_s p}{(b + p^n)^{1/n}} \quad (4)$$

Recently, Toth³¹ has himself verified the thermodynamic consistency of the model. By contrast with the Langmuir–Freundlich model, the Toth model is reduced to follow Henry's law.

The Henry isotherm is applicable for linear adsorption data²⁹

$$q^* = K p \quad (5)$$

where K is the Henry constant.

Table 11. Regression Results for the Synthetic Zeolites (Lancaster and Sigma) and Polymeric Sorbents

sorbent	Langmuir	Freundlich	Langmuir–Freundlich	Toth
5A zeolite Lancaster total SS 66.45	$R^2 = 94.76\%$ RSS = 3.485 SEE = 0.762 $q_s = 7.12 \pm 0.34$ $b = 68.8 \pm 29.8$	$R^2 = 97.04\%$ RSS = 1.965 SEE = 0.572 $K = 4.87 \pm 0.28$ $n = 0.110 \pm 0.014$	$R^2 = 99.69\%$ RSS = 0.205 SEE = 0.203 $q_s = 8.41 \pm 0.39$ $b = 2.24 \pm 0.52$ $n = 0.322 \pm 0.037$	$R^2 = 99.83\%$ RSS = 0.113 SEE = 0.150 $q_s = 9.09 \pm 0.50$ $b = 0.104 \pm 0.006$ $n = 0.219 \pm 0.027$
13X zeolite Lancaster total SS 97.01	$R^2 = 94.99\%$ RSS = 4.865 SEE = 0.900 $q_s = 8.52 \pm 0.41$ $b = 12.8 \pm 5.6$	$R^2 = 98.00\%$ RSS = 1.937 SEE = 0.568 $K = 5.36 \pm 0.30$ $n = 0.130 \pm 0.014$	$R^2 = 99.95\%$ RSS = 0.046 SEE = 0.096 $q_s = 11.0 \pm 0.3$ $b = 1.23 \pm 0.11$ $n = 0.313 \pm 0.015$	$R^2 = 99.99\%$ RSS = 0.010 SEE = 0.044 $q_s = 13.2 \pm 0.3$ $b = 0.151 \pm 0.002$ $n = 0.182 \pm 0.006$
5A zeolite Sigma total SS 53.56	$R^2 = 92.84\%$ RSS = 3.834 SEE = 0.740 $q_s = 6.72 \pm 0.28$ $b = 56.8 \pm 28.6$	$R^2 = 98.49\%$ RSS = 0.809 SEE = 0.340 $K = 4.75 \pm 0.18$ $n = 0.104 \pm 0.010$	$R^2 = 99.91\%$ RSS = 0.050 SEE = 0.091 $q_s = 8.79 \pm 0.37$ $b = 1.46 \pm 0.19$ $n = 0.271 \pm 0.021$	$R^2 = 99.94\%$ RSS = 0.029 SEE = 0.070 $q_s = 9.84 \pm 0.52$ $b = 0.118 \pm 0.003$ $n = 0.176 \pm 0.016$
13X zeolite Sigma total SS 102.0	$R^2 = 93.54\%$ RSS = 6.593 SEE = 0.971 $q_s = 8.18 \pm 0.44$ $b = 6.81 \pm 3.71$	$R^2 = 97.46\%$ RSS = 2.588 SEE = 0.608 $K = 4.70 \pm 0.32$ $n = 0.148 \pm 0.017$	$R^2 = 98.73\%$ RSS = 1.292 SEE = 0.464 $q_s = 10.3 \pm 1.6$ $b = 1.16 \pm 0.54$ $n = 0.331 \pm 0.079$	$R^2 = 99.05\%$ RSS = 0.971 SEE = 0.402 $q_s = 11.9 \pm 2.6$ $b = 1.67 \pm 0.02$ $n = 0.206 \pm 0.069$
Purolite MN200 total SS 26.37	$R^2 = 99.12\%$ RSS = 0.232 SEE = 0.182 $q_s = 12.0 \pm 2.1$ $b = 0.00784 \pm 0.00203$	$R^2 = 99.84\%$ RSS = 0.042 SEE = 0.077 $K = 0.199 \pm 0.015$ $n = 0.717 \pm 0.018$	$R^2 = 99.79\%$ RSS = 0.055 SEE = 0.096 $q_s = 78.9 \pm 236.0$ $b = 0.00241 \pm 0.00678$ $n = 0.740 \pm 0.088$	$R^2 = 99.48\%$ RSS = 0.137 SEE = 0.151 $q_s = 41.1 \pm 117.0$ $b = 15.0 \pm 29.8$ $n = 0.478 \pm 0.523$
Amberlyst 15 total SS 167.9	$R^2 = 95.52\%$ RSS = 7.522 SEE = 1.037 $q_s = 9.87 \pm 0.52$ $b = 11.4 \pm 3.8$ q_s (mmol g ⁻¹) b (kPa ⁻¹)	$R^2 = 95.82\%$ RSS = 7.017 SEE = 1.001 $K = 4.92 \pm 0.50$ $n = 0.189 \pm 0.026$ K (kPa ⁻¹) n (-)	$R^2 = 97.06\%$ RSS = 4.932 SEE = 0.907 $q_s = 13.7 \pm 3.9$ $b = 0.753 \pm 0.533$ $n = 0.364 \pm 0.118$ q_s (mmol g ⁻¹) b (kPa ⁻¹) n (-)	$R^2 = 97.50$ RSS = 4.194 SEE = 0.836 $q_s = 14.9 \pm 5.8$ $b = 0.238 \pm 0.040$ $n = 0.242 \pm 0.129$ q_s (mmol g ⁻¹) b (kPa ⁻¹) n (-)

Table 12. Regression Results for the Carbon Sorbents

sorbent	Henry	Langmuir	Freundlich	Langmuir–Freundlich	Toth
activated carbon Darco total SS 13.58	$R^2 = 87.16\%$ RSS = 1.743 SEE = 0.499 $K = 50.0 \pm 3.7$	$R^2 = 99.62\%$ RSS = 0.051 SEE = 0.092 $q_s = 7.24 \pm 0.44$ $b = 13.7 \pm 1.5$	$R^2 = 99.95\%$ RSS = 0.006 SEE = 0.032 $K = 250 \pm 8$ $n = 619 \pm 8$	$R^2 = 99.99\%$ RSS = 0.002 SEE = 0.020 $q_s = 22.3 \pm 6.0$ $b = 9.41 \pm 2.01$ $n = 0.702 \pm 0.026$	$R^2 = 99.96\%$ RSS = 0.005 SEE = 0.032 $q_s = 47.3 \pm 42.0$ $b = 5.51 \pm 2.10$ $n = 0.329 \pm 0.101$
charcoal Sigma total SS 28.56	$R^2 = 97.61\%$ RSS = 0.682 SEE = 0.292 $K = 59.8 \pm 2.2$	$R^2 = 99.87\%$ RSS = 0.036 SEE = 0.072 $q_s = 14.2 \pm 1.1$ $b = 6.12 \pm 0.69$	$R^2 = 99.97\%$ RSS = 0.007 SEE = 0.032 $K = 157.0 \pm 5.3$ $n = 774 \pm 8$	$R^2 = 99.98\%$ RSS = 0.005 SEE = 0.028 $q_s = 50.8 \pm 24.6$ $b = 2.75 \pm 1.17$ $n = 0.822 \pm 0.026$	$R^2 = 99.96\%$ RSS = 0.012 SEE = 0.044 $q_s = 82 \pm 111$ $b = 18.1 \pm 12.8$ $n = 0.445 \pm 0.184$
activated carbon Merck total SS 25.77	$R^2 = 99.92\%$ RSS = 0.020 SEE = 0.050 $K = 55.4 \pm 0.4$ K (kPa ⁻¹) $\times 10^{-3}$	q_s (mmol g ⁻¹) b (kPa ⁻¹) $\times 10^{-3}$	K (kPa ⁻¹) $\times 10^{-3}$ $n \times 10^{-3}$	q_s (mmol g ⁻¹) b (kPa ⁻¹) $\times 10^{-3}$ n (-)	q_s (mmol g ⁻¹) b (kPa ⁻¹) n (-)

The parameters of the isotherm models were estimated by minimizing the weighted sum of residual squares, i.e., the differences between the experimental and estimated sorbate concentrations.³² The objective function (Q) to be minimized was expressed as follows:

$$Q = \sum w(q^* - \hat{q}^*)^2 \quad (6)$$

Equally weighted concentrations ($w = 1$) gave the best fit. The objective function of the isotherm models was minimized by the Levenberg–Marquardt algorithm.

Estimated parameter values, confidence intervals, and regression statistics, such as the total sum of squares (SS), coefficient of determination (R^2), residual sum of squares (RSS), and standard error of estimate (SEE), are presented in Tables 9–12 for all of the sorbents. The Langmuir model does not usually give an accurate prediction of the ammonia equilibrium data for inorganic sorbents. The R^2 , RSS, and SEE values, which describe the goodness of fit, are poor. Only the equilibrium of silica gel 40 seems to fit well. However, the Langmuir model predicts correctly the equilibria of polymeric sorbent MN200, activated carbon

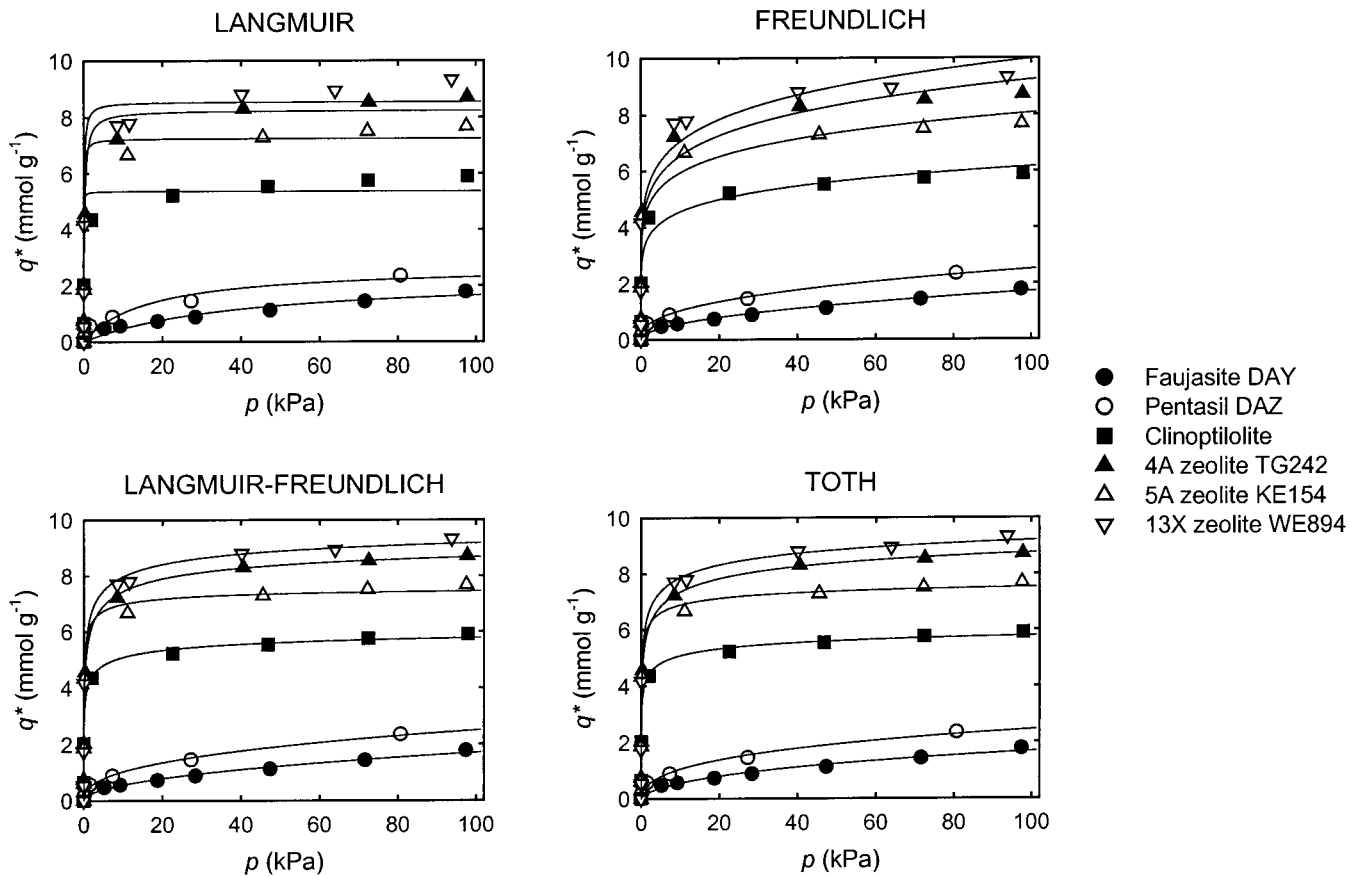


Figure 3. Experimental and predicted ammonia sorbate concentrations at equilibrium on the dealuminated, clinoptilolite, and Baylith zeolites.

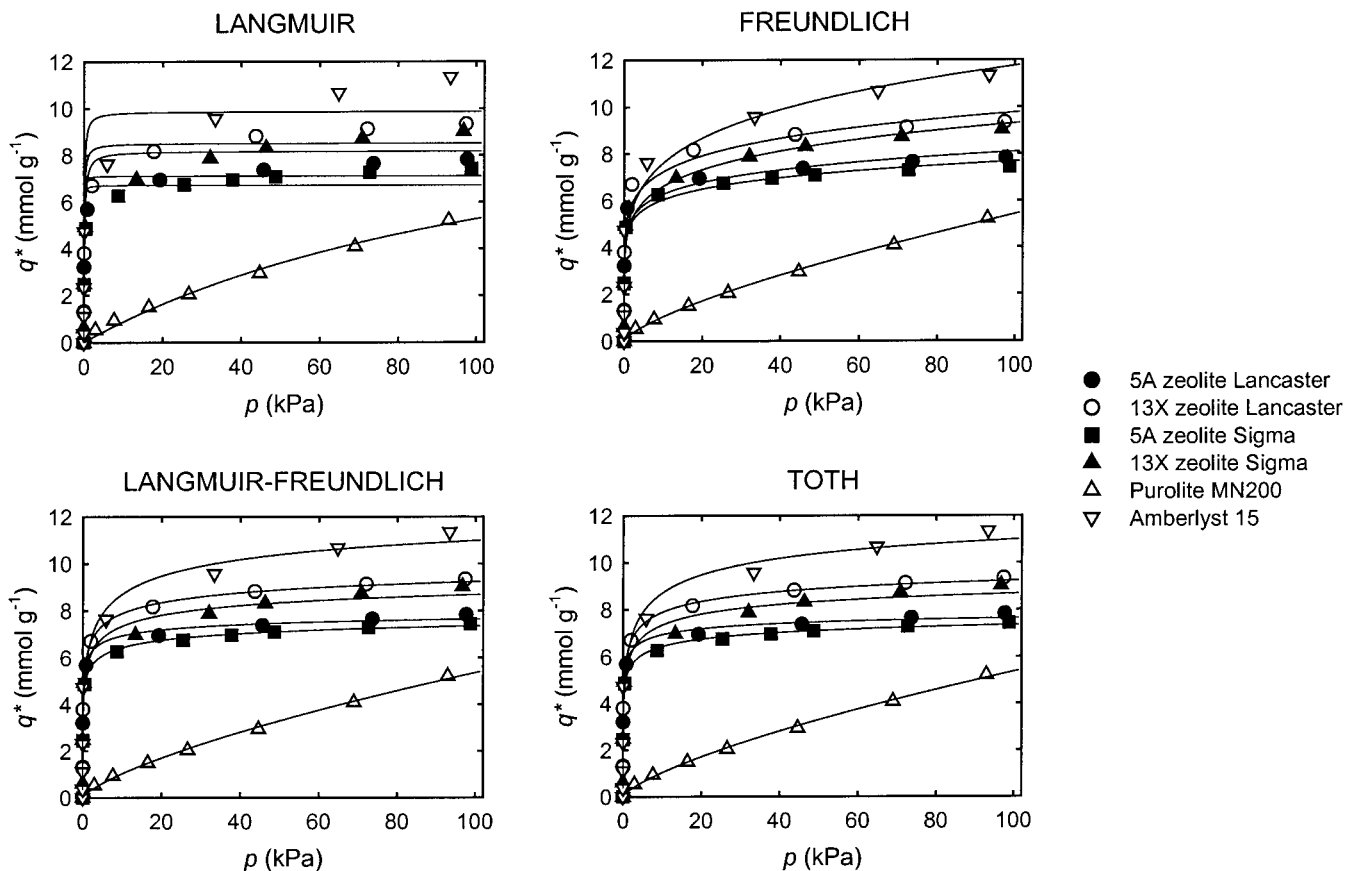


Figure 4. Experimental and predicted ammonia sorbate concentrations at equilibrium on the Lancaster and Sigma zeolites and polymeric sorbents.

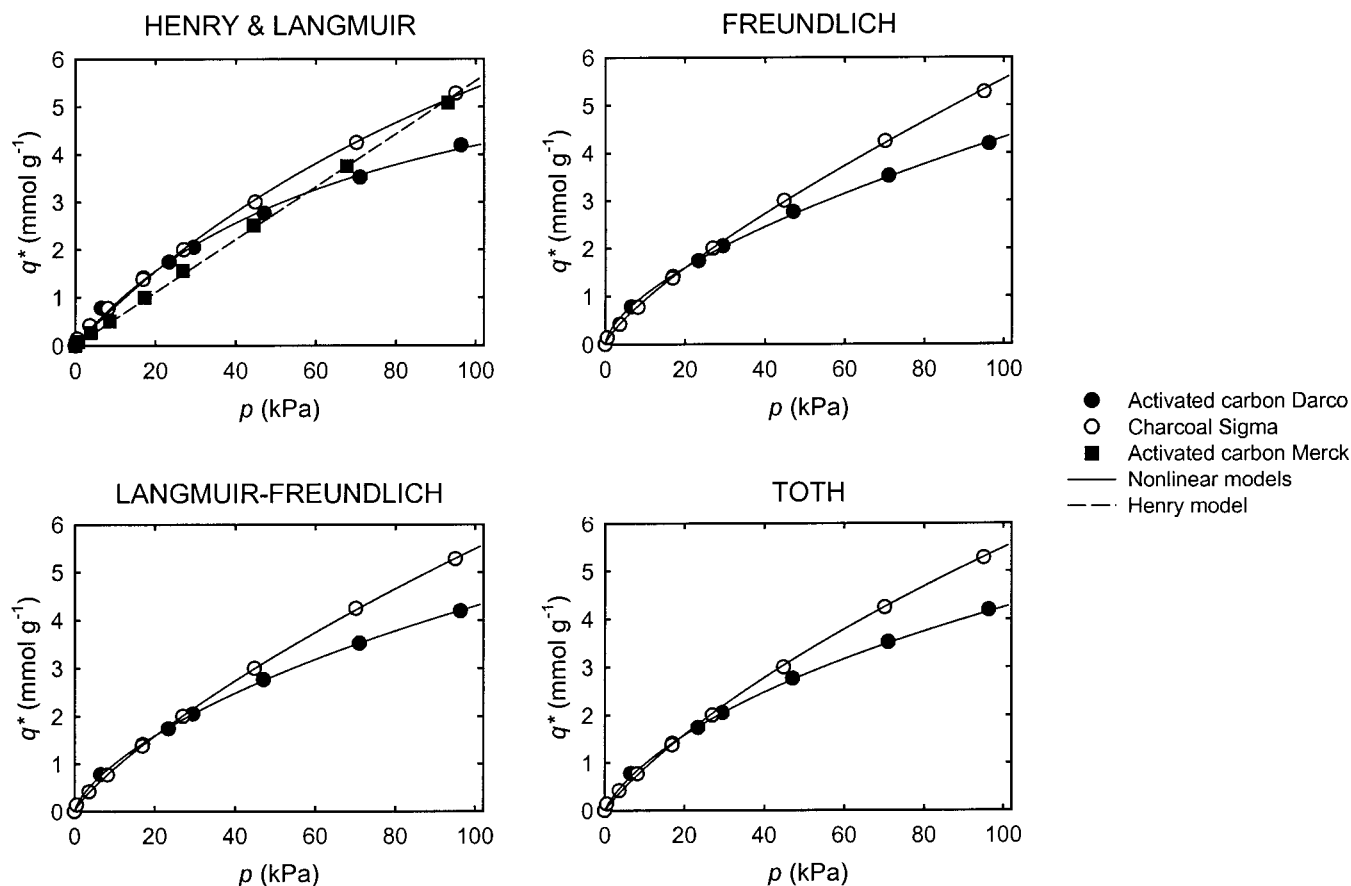


Figure 5. Experimental and predicted ammonia sorbate concentrations at equilibrium on the carbon sorbents.

Darco, and charcoal Sigma. The Freundlich model provides a better fit than the Langmuir model for the data of aluminas and silica gels 60 and 100. The fit of the Freundlich model is also better for the dealuminated zeolites, clinoptilolite, and zeolites of Lancaster and Sigma. In contrast, the Freundlich model correlates as well as the Langmuir model with the equilibria for silica gel 60, Baylith zeolites (TG242, KE154, and WE894), polymeric sorbents, and carbon sorbents. As expected, the three-parameter Langmuir–Freundlich and Toth models provide, in general, a better fit than the two-parameter models above. The Langmuir–Freundlich and Toth models are, in practice, equally accurate. If the R^2 , RSS, and SEE values are compared, the Langmuir–Freundlich and Toth models give the best fit for the following sorbents: alumina VPO2, alumina 1593, all silica gels, clinoptilolite, Baylith zeolites, Sigma zeolites, Lancaster zeolites, Amberlyst 15, and carbons. The R^2 value of 99% is regarded as a limit of superior correlation. The Amberlyst 15 and faujasite DAY are the only sorbents whose R^2 values for all models remain below 99%.

The confidence intervals of the estimated model parameters require further consideration. The goodness of fit alone does not guarantee the thermodynamical consistency of the isotherm model. If the estimated parameters are statistically reliable, namely, the confidence intervals are small, they are more probably thermodynamically consistent. For two-parameter isotherm models, the confidence interval of the parameters is always lower than the parameter estimate itself. The reliability of the parameters for the three-parameter models depends on the form of the isotherms. If the isotherm is favorable and contains a clear saturation level, then all three parameters can be estimated reliably. For example, the equilibria of 4A, 5A, and

13X zeolites have the saturation level at the upper pressure range, and thus the confidence intervals of the parameters for the Langmuir–Freundlich and Toth models are small (see Tables 11 and 12).

The fits of all models and experimental equilibrium data are depicted in Figures 2–5. The isotherm forms of silica gels, aluminas, and 4A, 5A, and 13X zeolites are highly favorable. In particular, the isotherm forms of 4A, 5A, and 13X zeolites are almost irreversible. They adsorb ammonia effectively at pressures of <0.02 kPa. The form of Amberlyst 15 is also favorable, but at low pressures, it is not as favorable as the 4A, 5A, and 13X zeolites. The isotherm forms of the other sorbents are only slightly favorable or linear. For the Langmuir–Freundlich and Toth models, the fits of the clearly distinguishable pressure range are as accurate as can be expected on the basis of the statistical values above. The Freundlich model works well with most of the sorbents. Its functional form is, however, too simple to predict the pressure range of the saturation level for 4A, 5A, and 13X zeolites. The same is also valid for the Langmuir model. In addition to zeolites, the Langmuir model fails in predicting the saturation level of aluminas and silica gels. The fits of highly favorable sorbents were compared at the pressures of <0.5 kPa and <0.02 kPa, even though the accuracy of low-pressure data is not as good as that at high pressure. The Langmuir–Freundlich and Toth models seem to give the best fit for the low-pressure data too.

Conclusion

The adsorption equilibria of ammonia gas were determined volumetrically at 298.15 K on inorganic and organic sorbents at pressures below 101 kPa. The polymeric

sorbent Amberlyst 15 provides the highest sorbate concentration at the highest pressures. The 4A, 5A, and 13X zeolites have lower sorbate concentrations near atmospheric pressure than Amberlyst 15, but the zeolites adsorb ammonia more effectively at low pressures. The difference between the zeolite grades obtained from the three suppliers was small. The equilibria of aluminas and silica gels are favorable for ammonia adsorption, but their ammonia capacity is much lower than that of the 4A, 5A, and 13X zeolites. At the experimental pressure range, the dealuminated zeolites, the nonsulfonated polymeric sorbent MN200, and the carbons have lower sorbate concentrations and less favorable, near linear, form isotherms when compared with the 4A, 5A, and 13X zeolites. The activated carbon Merck provides a pure linear equilibrium, and thus the Henry model gives the most accurate fit. The three-parameter Langmuir–Freundlich and Toth models are the best for most sorbents, especially, if the equilibrium data contain a saturation level. The two-parameter Freundlich model provides the most accurate fit for five of the 21 sorbents. The Langmuir model does not give the highest fit for any of the sorbents, although this model is regarded as thermodynamically more reliable.

Acknowledgment

The authors thank Bayer AG, Degussa AG, LaRoche Industries Inc., and Puralite International Ltd. for providing the sorbents.

Literature Cited

- King, C. J. *Separation Processes*; McGraw-Hill: New York, 1980.
- Ruthven, D. M.; Farooq, S.; Knaebel, K. S. *Pressure Swing Adsorption*; VCH: New York, 1994.
- Yang, R. T. *Gas Separation by Adsorption Processes*; Imperial College Press: London, 1997.
- Wankat, P. C. *Rate-Controlled Separations*; Elsevier: London, 1990.
- Knaebel, K. S. The Basics of Adsorber Design. *Chem. Eng.* **1999**, Apr, 92–101.
- Knaebel, K. S. For Your Next Separation Consider Adsorption. *Chem. Eng.* **1995**, Nov, 92–102.
- Markmann, B.; Mersmann, A. Prediction and Correlation of Multicomponent Adsorption Equilibria of Different Sized, Polar, and Polarizable Gases on Energetically Heterogeneous Adsorbents at High Pressures. In *Fundamentals of Adsorption*; Meunier, F., Ed.; Elsevier: Paris, 1998.
- Maurer, S.; Mersmann, A. Prediction of Henry's Law Constants for Gases and Vapors on Industrial Adsorbents. In *Fundamentals of Adsorption*; Meunier, F., Ed.; Elsevier: Paris, 1998.
- Lavie, R. Process for the Manufacture of Ammonia. U.S. Patent 4,537,760, 1985.
- Hirai, H.; Komiyama, M.; Kurima, K.; Wada, K. Adsorbent for Use in Selective Gas Adsorption Separation and a Process for Producing the Same. U.S. Patent 4,675,309, 1987.
- Knaebel, K. S. Pressure Swing Adsorption System for Ammonia Synthesis. U.S. Patent 5,711,926, 1998.
- Turunen, I.; Oinas, P. Process for the Preparation of Melamine. U.S. Patent 5,731,437, 1998.
- Valenzuela, D. P.; Myers, A. L. *Adsorption Equilibrium Data Handbook*; Prentice-Hall: Englewood Cliffs, NJ, 1989.
- Boki, K.; Tanada, S.; Nobuhiro, O.; Tsutsui, S.; Yamasaki, R.; Nakamura, M. Adsorption of Polar and Nonpolar Gases of Different Sizes on Nitrogen-Containing Activated Carbon. *J. Colloid Interface Sci.* **1987**, *120*, 286–288.
- Kuo, S.-L.; Pedram, E. O.; Hines, A. L. Analysis of Ammonia Adsorption on Silica Gel Using the Modified Potential Theory. *J. Chem. Eng. Data* **1985**, *30*, 330–332.
- Coughlan, B.; McCann, W. A. Adsorption Properties of Zeolitic Ruthenium and of Chromium, Iron and Lanthanum Mordenites. Part 1. Equilibria and Affinities. *J. Chem. Soc., Faraday Trans. 1* **1979**, *75*, 1969–1983.
- Shiralkar, V. P.; Kulkarni, S. B. Sorption of Ammonia in Cation-Exchanged Y Zeolites: Isotherms and State of Sorbed Molecules. *J. Colloid Interface Sci.* **1985**, *108*, 1–10.
- Hayhurst, D. T. Gas Adsorption by Some Natural Zeolites. *Chem. Eng. Commun.* **1980**, *4*, 729–735.
- Boddenberg, B.; Rakhmatkariev, G. U.; Viets, J. Thermodynamics and Statistical Mechanics of Ammonia in Zeolite NaZSM5. *Ber. Bunsen-Ges. Phys. Chem.* **1998**, *102*, 177–182.
- Schirmer, W.; Sichhart, K.-H.; Bülow, M.; Grossman, A. Zur Adsorption von Ammoniak an einem NaCaA-Zeolith. 2. Mitteilung: Kalorimetrische Bestimmung von differentiellen Adsorptionswärmen bei Temperaturen zwischen 23 und 300 °C (Adsorption of ammonia on a NaCaA zeolite. 2. Calorimetric determination of the differential heats of adsorption at temperatures between 23° and 300°). *Chem. Tech. (Leipzig)* **1971**, *23*, 476–478.
- Spindler, H.; Pape, D.; Preuss, H.; Entner, R. Adsorptionsgleichgewichtsmessungen von Ammoniak an 5A-Molekularsieben unter Druck (Adsorption equilibrium measurement of ammonia at 5 A molecular sieves under pressure). *Chem. Tech. (Leipzig)* **1990**, *42*, 432–433.
- Coughlan, B.; Shaw, R. G. Ion-Exchanged Zeolite A: Sorptive Properties of Carbon Dioxide and Ammonia—I. Sorbents and Sorption Equilibria. *Proc. R. Ir. Acad.* **1976**, *76B*, 191–210.
- Coughlan, B.; McEntee, J. J. Zeolitic Carbon Dioxide and Ammonia in Y-Type Molecular Sieves—I. Sorbents and Isotherms. *Proc. R. Ir. Acad.* **1976**, *76B*, 473–493.
- Coughlan, B.; Larkin, P. M. Physical Sorption in Transition Metal Loaded Molecular Sieves: Application of the Koble–Corrigan and Other Isotherm Equations to the Equilibria. *Proc. R. Ir. Acad.* **1977**, *76B*, 383–395.
- Chiachotni, K.; Heden, K.; Dushanov, D.; Minkova, V.; Rushev, D. Adsorption of Some Gases on Activated Carbon at High Pressure. *Izv. Khim.* **1991**, *24*, 420–428.
- Okamoto, J.; Sugo, T.; Fujiwara, K.; Sekiguchi, H. The Synthesis of a New Type Adsorbent for the Removal of Toxic Gas by Radiation-Induced Graft Polymerization. *Radiat. Phys. Chem.* **1990**, *35*, 113–116.
- Helminen, J.; Helenius, J.; Paatero, E.; Turunen, I. Comparison of Sorbents and Isotherm Models for NH₃–Gas Separation by Adsorption. *AIChE J.* **2000**, *46*, 1541–1555.
- Berlier, K.; Frère, M. Adsorption of CO₂ on Microporous Materials. 1. On Activated Carbon and Silica Gel. *J. Chem. Eng. Data* **1997**, *42*, 533–537.
- Ruthven, D. M. *Principles of Adsorption and Adsorption Processes*; Wiley: New York, 1984.
- Do, D. D. *Adsorption Analysis: Equilibria and Kinetics*; Imperial College Press: London, 1998.
- Toth, J. Some Consequences of the Application of Incorrect Gas/Solid Adsorption Isotherm Equations. *J. Colloid Interface Sci.* **1997**, *185*, 228–235.
- Haario, H. *MODEST Users Manual*; ProfMath Oy: Helsinki, 1994.

Received for review August 16, 2000. Accepted December 6, 2000. This work was supported by the Kemira Foundation, Kemira Chemicals Co., and the Finnish National Technology Agency (TEKES).

JE000273+